

OPTICAL PROPERTIES OF MICROCRYSTALLINE SILICON

MARTIN INGELS, MARTIN STUTZMANN, AND STEFAN ZOLLNER
Max-Planck-Institut für Festkörperforschung, D-7000 Stuttgart 80, FRG

ABSTRACT

Optical properties of undoped, microcrystalline silicon are investigated by photothermal deflection spectroscopy, spectroscopic ellipsometry and Raman scattering. Samples are prepared by recrystallization of hydrogenated amorphous silicon in the temperature range 680 – 900°C. The increase of grain sizes with increasing annealing temperature and the disappearance of amorphous tissue lead to noticeable changes in the observed spectra. It is argued that much of the pertinent structural information of $\mu\text{-Si}$ can be obtained by a suitable combination of optical measurements alone.

INTRODUCTION

Like hydrogenated amorphous silicon (a-Si:H) microcrystalline silicon ($\mu\text{-Si}$) appears to be a promising material for use in large area electronic devices. Both types of materials can be deposited at relatively low temperatures with the same deposition methods, e.g. plasma-enhanced chemical vapor deposition, but have quite different electronic, optical, and transport properties. A detailed understanding of these properties in $\mu\text{-Si}$ is complicated by the fact that the amorphous-to-microcrystalline transition occurs gradually: both, the volume fractions of amorphous versus microcrystalline material as well as the crystallite size in the $\mu\text{-Si}$ fraction are known to vary almost continuously as a function of deposition parameters such as substrate temperature, hydrogen dilution, gas residence times in the deposition reactor, etc. [1–3]. Therefore, in general many different experimental techniques probing structural and electronic properties are necessary for a sufficient characterization of any given $\mu\text{-Si}$ sample. Since such a complete characterization is in many cases not practical, it is useful to try to establish correlations between structural (Raman, x-ray, TEM) and electronic properties of $\mu\text{-Si}$ [4,5]. In the following, we will describe our attempts to test the applicability of such correlations to recrystallized a-Si:H samples.

EXPERIMENTAL DETAILS

$\mu\text{-Si}$ has been obtained by annealing a-Si:H samples at different temperatures between 300 and 900°C. Amorphous silicon samples were deposited by glow-discharge decomposition of silane at 230°C onto quartz substrates. Two different films thicknesses (0.5 and 1.5 μm) were used to check for possible influences of this parameter on the results. All samples were nominally undoped. Optical absorption data in the energy range 0.4 – 5.6 eV have been recorded by a combination of photothermal deflection spectroscopy [6], standard transmission measurements, and spectroscopic ellipsometry [7]. Raman spectra were obtained with an Ar⁺ ion laser ($\lambda = 5145 \text{ \AA}$) and a double monochromator, using a photon-counting system.

RESULTS AND DISCUSSION

Figure 1 shows a summary of the optical absorption spectra of a-Si:H, a-Si (after hydrogen evolution at 650°C), $\mu\text{-Si}$ just after thermal crystallization (685°C), and polycrystalline silicon on sapphire (SOS). In the case of high-quality a-Si:H ([H] \approx 10 at.%), the absorption coefficient, α , is high for $\hbar\omega > 3 \text{ eV}$ ($\alpha \approx 10^6 \text{ cm}^{-1}$) and connects smoothly with the exponential Urbach tail region ($1.5 \text{ eV} \leq \hbar\omega \leq 2 \text{ eV}$). For $\hbar\omega < 1.5 \text{ eV}$, the defect absorption band of the midgap dangling bond defect levels is visible ($N_D \approx 10^{16} \text{ cm}^{-3}$). Upon desorption of the bonded hydrogen, the defect absorption increases by about two

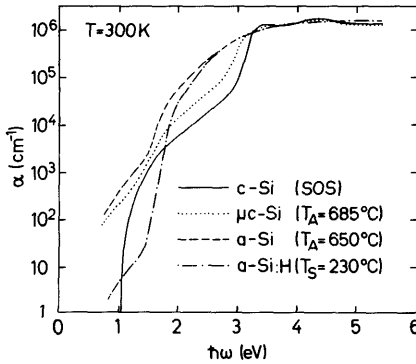


Fig. 1 Optical absorption coefficient as a function of energy for crystalline silicon on sapphire (solid curve), μ c-Si (dotted curve), amorphous silicon (dashed curve) and hydrogenated amorphous silicon (dash-dotted curve).

orders of magnitude (i.e. 10^{18} cm^{-3}). In addition, the optical absorption in the Urbach tail region and the visible part of the optical spectrum increases (dashed line in Fig. 1). After crystallization of the sample at $T_A = 685^\circ\text{C}$, the absorption in the visible region of the spectrum decreases by about a factor of four as the indirect character of the optical transitions in this energy range is reestablished. At higher photon energies, the absorption spectra of microcrystalline Si develop the two-peak structure caused by the direct transitions across the E_1 and E_2 gaps in the Si band structure. However, in this logarithmic scale there is little difference between the absorption coefficient for $\hbar\omega > 3.5 \text{ eV}$ in all four samples shown in Fig. 1.

The more interesting spectral region below $\hbar\omega \approx 3 \text{ eV}$ is shown in detail in Fig. 2. The dotted curves indicate the two extreme cases of pure amorphous silicon obtained by annealing at 675°C , and of crystalline Si. Absorption coefficients for μ c-Si always fall between these two limits. As the annealing temperature for the μ c-Si is raised from 685 to 800°C , the absorption above 1.7 eV decreases slightly, whereas that at lower photon energies increases again. We attribute the annealing-induced decrease of the absorption coefficient in the region $1.7 \text{ eV} \leq \hbar\omega \leq 3 \text{ eV}$ mainly to a decrease of the volume fraction of amorphous inter-grain tissue, which occurs when the microcrystallites grow from typically 80 \AA diameter just after crystallization to about 130 \AA diameter after annealing at 900°C (see below). k -uncertainty due to the finite size of the crystallites appears to be less important in this energy range [8].

An interesting point is that the absorption in the subgap region ($\hbar\omega \leq 1.3 \text{ eV}$) in-

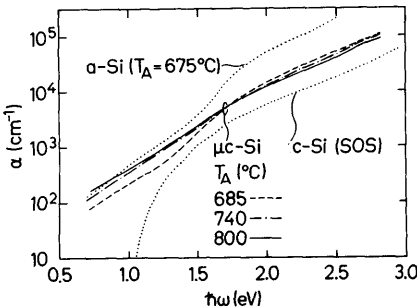


Fig. 2 Absorption coefficient in the range 0.6 eV to 3 eV for microcrystalline silicon annealed at different temperatures. The absorption coefficients for amorphous and crystalline silicon are included for comparison (dotted lines).

creases with increasing annealing temperature. Based on a study of polycrystalline silicon, it was suggested by Jackson et al. [9], that the subgap absorption, as in amorphous silicon, is a measure for the density of grain boundary defect states (dangling bonds). However, it is known that the dangling bond density as determined by electron spin resonance actually decreases upon annealing of undoped $\mu\text{-Si}$. Also, hydrogen passivation is known to strongly reduce the density of ESR centers in $\mu\text{-Si}$ [10], but is causes only small changes in the subgap absorption [9,11]. These results indicate that the connection between subgap absorption and dangling bond defect density in $\mu\text{-Si}$ appears to be less straightforward than originally believed. Apparently there is a large, approximately constant density of spinless defects which contribute to the subgap absorption.

For a structural characterization of our samples (amorphous fraction, crystallite size) we have used Raman scattering, and some characteristic spectra obtained before and after crystallization are depicted in Fig. 3. Up to an annealing temperature of 650°C , all samples remain amorphous, with little change in the Si vibrational density of states. The main structural change in this temperature range is the loss of bonded hydrogen, which gives rise to the broad Raman peak around 2000 cm^{-1} . For the sample in Fig. 3, crystallization occurs at 675°C . However, the silicon optical phonon peak at $\approx 520\text{ cm}^{-1}$ is quite broad (FWHM 10 cm^{-1}), and there exists still a noticeable fraction of amorphous tissue as indicated by the low energy shoulder in the Raman spectrum around 480 cm^{-1} . The grain size can be estimated from the width of the phonon peak and the peak position to about $70\text{ \AA} \pm 20\text{ \AA}$ just after crystallization [12]. Upon annealing at 900°C , the amorphous fraction disappears almost completely and the phonon peak narrows and shifts towards higher energies, indicating further growth of microcrystallites to a size of $\approx 120\text{ \AA} \pm 20\text{ \AA}$, in agreement with x-ray diffraction spectra obtained for the same samples. However, the Raman peak width is still considerably larger than that of the silicon-on-sapphire (SOS) sample used as a reference for c-Si.

It is known from the literature that the crystallite size in $\mu\text{-Si}$ can also be estimated from the broadening of the E_1 -optical transition at $\hbar\omega \approx 3.4\text{ eV}$ [5]. In order to test

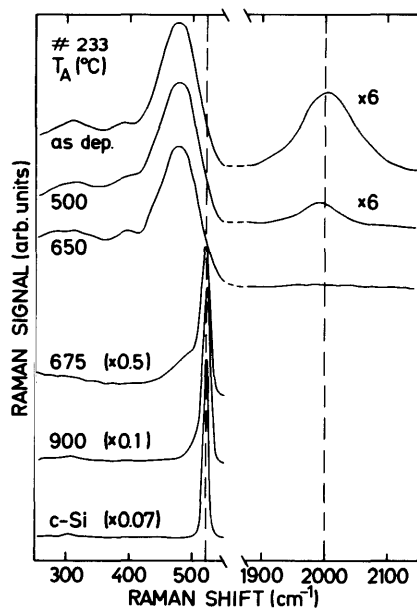


Fig. 3 Raman spectra of sample #233 after anneal at different temperatures.

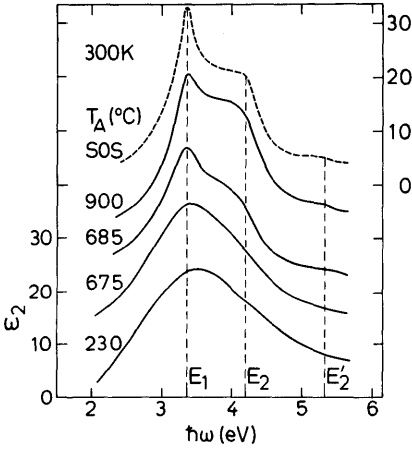


Fig. 4 Room temperature spectra of the imaginary part, ϵ_2 , of the dielectric constant. Spectra are determined by spectroscopic ellipsometry and are shown for different annealing stages. The spectrum of SOS is included for comparison (dashed curve).

this for the present samples, we have measured the pseudo-dielectric constants ϵ_1 and ϵ_2 by spectroscopic ellipsometry in the energy range $2 \text{ eV} < \hbar\omega < 5.6 \text{ eV}$. The results obtained for the imaginary part $\epsilon_2(\hbar\omega)$ of the dielectric constant as a function of energy are shown in Fig. 4. As long as the sample remains amorphous, the ϵ_2 -spectra consist of a single broad peak around $\hbar\omega \approx 3.5 \text{ eV}$. Crystallization of the sample becomes noticeable by a change to a more structured spectrum between $T_A = 675^\circ\text{C}$ (amorphous) and $T_A = 685^\circ\text{C}$ ($\mu\text{-Si}$). In particular, the peaks corresponding to direct optical transitions between the highest valence band and the lowest conduction band become visible: the $E_1(E'_0)$ peak caused by the almost parallel bands between the Γ - and the L-point, and the E_2 peak at $\hbar\omega \approx 4.2 \text{ eV}$ due to optical transitions at the X-point of the Brillouin zone. With increasing crystallite size one observes a decreasing width, Γ , of the E_1 -transition. For a more quantitative analysis, we have extracted Γ by fitting the second derivative of the dielectric function, $d^2\epsilon_2/d(\hbar\omega)^2$, to the theoretically expected form for a two-dimensional critical point in the c-Si band structure [13]

$$\frac{d^2\epsilon_2}{d(\hbar\omega)^2} \propto \text{Im} \{ (\hbar\omega - E_1 + i\Gamma)^{-2} \}. \quad (1)$$

The obtained values for the peak width $\Gamma(E_1)$ are plotted in Fig. 5 versus the optical phonon linewidth, Γ_{TO} , deduced from the Raman spectra. Over the limited range of crystallite sizes investigated in this study, we find a roughly linear dependence between the two quantities in Fig. 5, with $\Gamma(E_1) \approx 160 \text{ meV}$ for the smallest crystallites just after crystallization ($\approx 80 \text{ \AA}$ diameter) and $\Gamma(E_1) \approx 70 \text{ meV}$ for SOS, in agreement with room temperature values for bulk crystalline silicon [13]. With a suitable calibration, it should therefore be possible to estimate crystallite sizes in $\mu\text{-Si}$ solely from optical data obtained in the spectral region of the E_1 -transition, without the necessity for more direct structural measurements (Raman, x-ray diffraction, or electron microscopy). However, to this end a more extensive data base would be desirable.

We would like to thank R. Arce for his help with sample preparation and M. Brunel (CNRS, Grenoble) for the x-ray diffraction measurements. Valuable discussions with E. Bustarret are gratefully acknowledged. We also thank M. Brandt and C. Herrero for a critical reading of the manuscript.

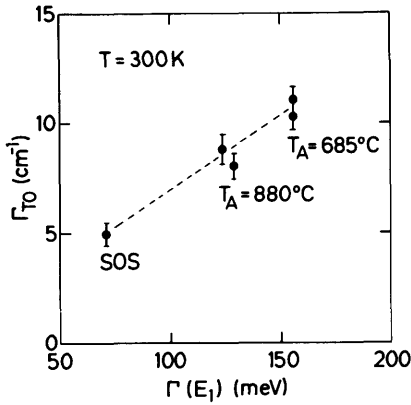


Fig. 5 Correlation between the width Γ_{TO} of the optical phonon Raman peak and the width parameter $\Gamma(E_1)$ of the E_1 -transition at 3.4 eV.

REFERENCES

- [1] Z. Iqbal, S. Vepřek, *J. Phys. C* **15**, 377 (1982).
- [2] Y. Mishima, S. Miyazaki, M. Hirose, Y. Osaka, *Phil. Mag. B* **46**, 1 (1982).
- [3] N.M. Johnson, S.E. Ready, J.B. Boyce, C.D. Doland, S.H. Wolff, J. Walker, *Appl. Phys. Lett.* **53**, 1626 (1988).
- [4] S. Kumar, D.K. Pandya, K.L. Chopra, *J. Appl. Phys.* **63**, 1497 (1988).
- [5] S. Logothetidis, *J. Appl. Phys.* **65**, 2416 (1989).
- [6] W.B. Jackson, N.M. Amer, A.C. Boccara, D. Fournier, *Appl. Optics* **20**, 1333 (1981).
- [7] D.E. Aspnes, A.A. Studna, *Appl. Optics* **14**, 220 (1975).
- [8] M.A. Hachicha, E. Bustarret, this volume.
- [9] W.B. Jackson, N.M. Johnson, D.K. Biegelsen, *Appl. Phys. Lett.* **43**, 195 (1983).
- [10] S. Hasegawa, S. Takenaka, Y. Kurata, *J. Appl. Phys.* **53**, 5022 (1982).
- [11] M. Stutzmann, C.P. Herrero, M. Ingels, A. Breitschwerdt, this volume.
- [12] I.H. Campbell, P.M. Fauchet, *Solid State Commun.* **58**, 739 (1986).
- [13] P. Lautenschlager, M. Garriga, L. Viña, M. Cardona, *Phys. Rev. B* **36**, 4821 (1987).